Green Synthesis and Bioactivities of Silver Nanoparticles Derived from *Mercurialis annua* L. Extract

Aisha Mohamud Salad [a], and Zeynep Akar [b,*]

Biogenic synthesis using plant materials provides a sustainable alternative to classical nanoparticle fabrication, minimizing chemical hazards and decreasing energy input. In this study, silver nanoparticles (AgNPs) were prepared using an aqueous extract of *Mercurialis annua* and characterized. Physicochemical properties of the AgNPs were confirmed using ultraviolet–visible spectroscopy (UV–Vis), Fourier transform infrared (FTIR) analysis, X-ray diffraction (XRD), and transmission electron microscopy coupled with energy-dispersive X-ray (TEM–EDX), which collectively indicated crystalline, spherical silver nanoparticles stabilized by extract-derived functional groups. Subsequently, the biological activities of both the nanoparticles and the extract were comparatively evaluated using antioxidant tests, including cupric ion reducing antioxidant capacity (CUPRAC), ferric reducing antioxidant power (FRAP), 2,2-diphenyl-1-picrylhydrazyl (DPPH), total phenolic content (TPC), and total flavonoid content (TFC), as well as enzyme inhibition tests targeting α-glucosidase and carbonic anhydrase. Liquid chromatography-mass spectrometry profiling identified 31 phenolic constituents in the extract, with ferulic, caffeic, salicylic, and 4-hydroxybenzoic acids detected in high abundance. Overall, the biosynthesized AgNPs demonstrated higher antioxidant performance and stronger inhibitory effects on both enzymes compared with the crude extract. These results indicate that *M. annua*-based AgNPs hold considerable promise sustainable and effective bioactive agents for future biomedical and biotechnological applications.

DOI: 10.15376/biores.21.4.9492-9512

Keywords: α-Glucosidase; Antioxidant activity; Carbonic anhydrase; LC-MS/MS; Mercurialis annua

Contact information: a: Department of Biotechnology, Graduate Education Institute, Gümüshane University, Gümüshane, Türkiye; b: Department of Occupational Health and Safety, Faculty of Health Sciences, Gümüshane University, Gümüshane, Türkiye;
** Corresponding author: zeynep_iskefiyeli@hotmail.com*

INTRODUCTION

Silver nanoparticles, characterized by their ultra-small size and the resulting high surface area and increased reactivity, have broad application potential across various fields, particularly in health and environmental research (Aktepe *et al*. 2025a; Ahmed *et al*. 2016; Jiang *et al*. 2025). However, commonly used physical and chemical synthesis methods involve high energy consumption and toxic chemical release, posing environmental and health concerns (Iravani *et al*. 2014), whereas green synthesis using biological materials provides a sustainable and cost-effective alternative (Sharma *et al*. 2019; Karakullukçu *et al*. 2023; Singh *et al*. 2023).

An increasingly popular, environmentally sustainable, and eco-friendly strategy for metallic nanoparticle production involves harnessing various biological sources, such as

plants, fungi, algae, bacteria, yeasts, and other microorganisms (Cardoso *et al.* 2025). Plants contain diverse phytochemical compounds, including phenols, terpenes, alkaloids, saponins, proteins, and carbohydrate-based molecules that function as both reducing and stabilizing agents during metal nanoparticle formation; in addition, microorganisms provide key enzymatic systems that function simultaneously as reducing and stabilizing components (Ovais *et al*. 2018). Biomolecules act as reducing and stabilizing agents, modifying nanoparticle surfaces through capping and influencing their biological activity (Hanna *et al*. 2025). Furthermore, the characterization and identification of bioactive compounds as part of green synthesis processes is of significant importance. Accordingly, many studies have investigated the bioactive potential of silver nanoparticles (AgNPs), encompassing their anticancer, enzyme-inhibitory, antioxidant, and antimicrobial effects (Rai *et al*. 2009). Thus, oxidative stress and rising antimicrobial resistance have increased interest in natural bioactive compounds (Akar *et al*. 2020).

In recent years, plant-based natural products have gained increasing attention owing to their low toxicity, diverse biological activities, and economic significance (Tekin *et al*. 2025). Among these, vascular plants (Tracheophyta) are frequently chosen for the green fabrication of nanoparticles because of the high diversity and abundance of biologically active compounds they contain (Smitha *et al*. 2020). These compounds, particularly flavonoids and anthocyanins, are widely distributed in plants and are associated with biological activity (Alan and Çolak 2025; Aktepe *et al*. 2025b). In this study, *Mercurialis annua* L., a traditional medicinal plant due to its active compounds, was chosen as the green synthesis agent. *M. annua*, a dioecious annual wild herb belonging to the Euphorbiaceae plant family, is common in disturbed and agricultural areas (Pannell *et al*. 2008). *M. annua*, traditionally used in European herbal medicine since ancient times, has been applied for the treatment of wounds, burns, and a range of digestive and gynecological disorders due to its richness in bioactive secondary metabolites (Lorenz *et al*. 2012). *M. annua*, known to be rich in bioactive secondary metabolites, was considered a suitable research material for investigating the bioactivity of plant extracts and AgNPs obtained from the extracts, primarily due to its high phenolic content, wide availability, and documented use in traditional European medicine.

This study focused on characterizing the physicochemical properties of AgNPs synthesized *via* a green method using *M. annua*, comparing the antioxidant capacities of the plant extract and AgNPs using multiple analytical approaches, evaluating their inhibitory effects on α-glucosidase and carbonic anhydrase (CA), and profiling the chemical constituents of the extract using liquid chromatography-tandem mass spectrometry (LC–MS/MS). Accordingly, it provides new insights into the green synthesis of silver nanoparticles using *M. annua* and the evaluation of their biological activities.

EXPERIMENTAL

Preparation of Plant Extract

Mercurialis annua was collected in March 2025 from the Darıca neighbourhood of Akçaabat district, Trabzon, Türkiye. The plant was shade-dried, and its aerial parts were ground into powder. A total of 30 g of powders were combined with 0.2 L of distilled water and left for one day and under continuous mixing at 27 °C. The resulting solution was passed *via* sequential filtering papers with varying pore diameters to clarify the extract, then stored at +4 °C until use in bioactivity assays and AgNP production.

Synthesis of Silver Nanoparticle (AgNP) Using Plant Extract

The experimental conditions were selected in accordance with commonly reported methods for the green synthesis of silver nanoparticles. A 10 mM $AgNO_3$ solution with a volume of 90 mL was first prepared, and 10 mL of the plant extract was gradually added to the reaction mixture. As the process continued, the solution gradually adopted a darker color, indicating AgNP formation as a result of surface plasmon resonance (SPR). The suspension was then maintained under magnetic stirring for a further 4 h. Once AgNP formation was verified spectrophotometrically, the suspension was processed in a centrifuge at 12,000 rpm for 10 min. This purification phase was conducted twice using pure water and ethanol under the same centrifugation conditions. Finally, the collected AgNPs were transferred to a tube and dried, resulting in successful silver nanoparticle production (Akar *et al*. 2024).

Structural Analysis of AgNPs

For the ultraviolet–visible measurements (Uv-Vis), a Shimadzu UV-1800 instrument (Japan) was used. Aliquots of the synthesized AgNPs and the aerial parts of the extracts were placed into quartz cuvettes, and the spectra were recorded at ambient temperature across the 200 to 800 nm range with a bandwidth resolution of 1.0 nm

Fourier transform infrared spectroscopy (FTIR) was performed to investigate the chemical associations occurring between the extract and the AgNPs produced through extract-mediated synthesis. The aim was to determine the functional groups contributing to silver-ion reduction and nanoparticle surface stabilization. Spectral recordings were collected within the 4000 to 4500 cm^{-1} range using an FTIR spectrometer (Brand: Perkin Elmer, Model: UART Two).

X-ray diffraction (XRD) served to evaluate the lattice configuration and phase behavior of the AgNPs fabricated using the plant extract. Crystallinity was determined through the analysis of the obtained diffraction signals. Measurements were conducted using a Bruker D8 Discover Diffractometer at the Central Research Laboratory of Bayburt University. The XRD scans were measured in the 2θ range of 10° to 80°, and the collected data were used for the analysis of the diffraction patterns.

Morphological features and the elemental profile of the AgNPs were analyzed using Transmission Electron Microscopy (TEM) at the Central Research Laboratory of Bayburt University, employing an FEI Talos F200S instrument operated at 200 kV. Before imaging, the nanoparticles were suspended in ethanol, applied onto a Cu grid, and dried under vacuum. Elemental profiling was achieved through the Energy-Dispersive X-ray Spectroscopy (EDX) detector integrated into the TEM system.

Biological Activity Assays

Antioxidant activity assays

2,2-Diphenyl-1-picrylhydrazyl (DPPH) is a stable, commercially supplied radical commonly used in antioxidant assays, showing a characteristic absorption maximum at 517 nm (Brand-Williams 1995). A DPPH solution adjusted to 100 µM prepared in methanol was used in the assay. Initial concentrations of the samples were determined through a series of preliminary tests using the plant extract and silver nanoparticles. For the reaction mixture, an equal volume of a DPPH stock at 100 µM was combined with a 750-µL portion of each sample. After allowing the solution to settle for 50 min, the absorbance in the UV range was measured at 517 nm. Changes in DPPH absorbance were assessed for samples

prepared at varying concentrations. The level requirement to reducing the initial DPPH signal at 50% was calculated (mg/mL) using the linear regression equation $y = ax + b$, and this resulting value was reported as SC_{50}. A lower SC_{50} reflects stronger radical-scavenging capacity.

In accordance with the ferric reducing antioxidant power (FRAP) protocol outlined by Benzie and Strain (1996), both the *M. annua* extract and the AgNPs produced using this extract were assessed for their antioxidant capacity. Trolox® served as the standard compound, and a calibration curve was generated using solutions at 1000, 500, 250, 125, 62.5, and 31.25 µM (Benzie and Strain 1996). At the beginning of the procedure, 50 µL volumes of the specimens or standards were put into the reaction tubes. After this step, 1500 µL of the FRAP solvent mixture (60% methanol in purified water) was dispensed into the tubes, as followed in the subsequent addition of an identical volume of freshly prepared FRAP reagent. The reaction tubes were vortexed and then remained at standard room conditions for 20 min. After this period was completed, absorbance at 595 nm was recorded for each sample. The antioxidant activity of samples was quantified based on its Trolox-equivalent value and reported in µM TEAC units.

Cupric ion reducing antioxidant capacity (CUPRAC) analysis was performed according to Apak (2004) with minor modifications from Akar *et al*. (2021). In the CUPRAC assay, Cu (II) chloride, neocuproine (prepared in 96% ethanol), the pH-7 ammonium acetate buffer, and the sample solutions were mixed at identical volumes. The reaction mixture was subsequently adjusted until the overall volume reached 4.1 mL. The reaction mixtures were incubated in closed tubes at room standard room conditions for 30 min, and at 450 nm, their absorbance was then measured. Antioxidant capacity (µM TEAC) was calculated using a Trolox calibration graph prepared from solutions up to 1000 µM.

An adapted Folin–Ciocalteu protocol, based on Slinkard and Singleton (1977), was used to evaluate the total phenolic content. To begin the assay, 0.05 mL of sample was first mixed with 2.5 mL of deionized water. The mixture was supplemented with 0.25 mL of 0.2 N Folin–Ciocalteu reagent and subsequently with 0.75 mL of 7.5% Na_2CO_3 solution, after which vortexing was performed. Following preparation, the mixed samples were stored at standard room condition for 2 h before measurement. A reading of absorbance was taken at 765 nm. For quantification, gallic acid solutions prepared at concentrations up to 0.5 mg/mL were used to construct the calibration plot. Phenolic levels in the samples were determined based on the calibration curve equation.

Flavonoid levels were assessed using a modification of the method previously developed by Fukumoto and Mazza (2000). This study was conducted with three parallel samples, sample, and reagent controls prepared. Equal volumes of the specimens were pipetted into tubes and mixed with methanol. Then, a solution of ammonium acetate at 1 M concentration, together with aluminum nitrate at 10% strength, was mixed with the solutions. The mixtures were subjected to an incubation period of 40 min, after which time the absorbances were measured at a wavelength of 415 nm. Quercetin was used as the standard compound. It was prepared at five different concentrations (starting at 0.25 mg/mL). Quercetin equivalents (QAE µg/mL) were used to quantify the flavonoid levels in both the plant extract and the plant-derived AgNPs.

Enzyme inhibition activities

A modified form of the Yu *et al*. (2012) protocol was employed. In this setup, each reaction tube was first supplied with 650 µL of phosphate-based buffer prepared at 0.1 M and pH 6.8. Subsequently, the reaction was supplemented with 20 µL of the sample

followed by 30 µL of α-glucosidase—isolated from *Saccharomyces cerevisiae* and supplied as a lyophilized enzyme (≥ 10 U/mg protein). The obtained mixture was maintained at 37 °C for 10 min. Afterward, 0.75 µL of the pNPG substrate (4-nitrophenyl-α-D-glucopyranoside) was pipetted into each tube. Then, it was added; the tubes were kept again under 37 °C conditions for an additional 15 min. To stop the reaction, each tube was supplemented with 650 µL of 1 M Na_2CO_3. Upon substrate addition, incubation was continued at 37 °C for an additional 15 min. The reaction was stopped by introducing 650 µL of the 1 M Na_2CO_3 solution into each tube. For each mixture, the 405-nm absorbance was recorded using a UV–Vis system. Acarbose, prepared in varying concentrations, was used as the reference inhibitor. All assays were performed in three independent replicates, and reagent and sample blanks were also prepared. The IC_{50} values, representing the concentrations of substances that halve enzyme activity, were calculated for acarbose and the tested samples.

Bovine carbonic anhydrase (BCA; lyophilized, ≥ 3,500 W-A units/mg protein) served as the enzyme for evaluating the inhibition efficiency of the samples.

Esterase activity method

Samples were analyzed for their ability to inhibit carbonic anhydrase (CA), with bovine carbonic anhydrase serving as the enzyme source. During the process, p-nitrophenyl acetate (PNPA) is broken down by carbonic anhydrase to form p-nitrophenol and p-nitrophenolate ions (Armstrong and Frederick 1966). For esterase activity measurement, 1.1 mL of Tris–SO_4 buffer (0.05 M, pH 7.4), 1.5 mL of a 3 mM p-nitrophenyl acetate solution, and a mixture of 300 µL enzyme solution with 100 µL distilled water were assembled to form the reaction medium. The progress of the reaction was monitored spectrophotometrically, with absorbance readings taken at 348 nm over time. The IC_{50} value of sulfanilamide (the concentration in the sample that halves the enzyme activity) was calculated.

Phenolic Content of Plant Extract and Silver Nanoparticle by LC-MS/MS

The liquid chromatography-tandem mass spectrometry (LC–MS/MS) based phenolic profiling was performed at Hitit University's Scientific and Technical Application and Research Center using a Thermo Scientific Dionex Ultimate 3000 system coupled to a TSQ Quantum detector. Ethanol extracts of *M. annua* leaves, stems, and flowers (aerial parts) were analyzed. Chromatographic separation was achieved on an ODS Hypersil column (4.6 × 250 mm^2, 5 µm) using a gradient composed of water with 0.1% formic acid (solvent A) and methanol (solvent B). The injection volume was 20 µL, the column temperature was maintained at 30 °C, and the mobile phase was delivered at a flow rate of 0.7 mL/min. The gradient began with 100% A, reached 5% A at 22 min, and transitioned to 100% B at 26 min, where it was held for 8 min.

Validation and Statistical Analysis

Standard solutions and plant extracts were analyzed at five concentration levels, each tested in triplicate, to construct the curves used for antioxidant and enzyme activity assessments. In the course of the biological activity tests of standards, the plant-derived extracts and the synthesized AgNPs, the R^2 values were generally observed to exceed 0.9900. The Student's t-test was applied to assess differences between extract and AgNP samples, where $p < 0.05$ indicated statistical significance.

RESULTS AND DISCUSSION

Structural Analysis of AgNPs

Evidence for AgNP formation was provided by the UV–Vis spectral profile as well as the distinct color change observed in the reaction mixture. Addition of the plant extract to the Ag^+ solution revealed a brown-to-red color shift, recognized as the earliest and most rapid visual confirmation of AgNP formation. Following this, UV–Vis spectrophotometric analysis was conducted, which provided further evidence to support the occurrence of colloidal AgNPs, as shown by their characteristic absorption behavior. Spectrophotometric scans were performed in the 200 to 800 nm range for both the plant extract and the AgNP solution (Fig. 1). The presence of the surface plasmon resonance (SPR) band detected in the UV–Vis profile indicated that the AgNPs effectively formed. Nanoparticle size, morphology, surface charge, and surrounding medium collectively determine the position and amplitude of the SPR response. Surface plasmon resonance occurs as incoming light triggers the coordinated movement of conduction electrons across the nanoparticle surface, an effect enhanced by functional groups including $–NH_2$, –OH, and –COOH. As illustrated in Fig. 1, A distinct SPR band appeared near 450 nm in the UV–Vis profile of the AgNPs. This result corresponds to previous findings on biosynthesis of silver nanoparticles using plant extracts and confirms that AgNPs were successfully produced (Henglein 1993; Özçelik and Kara 2023).

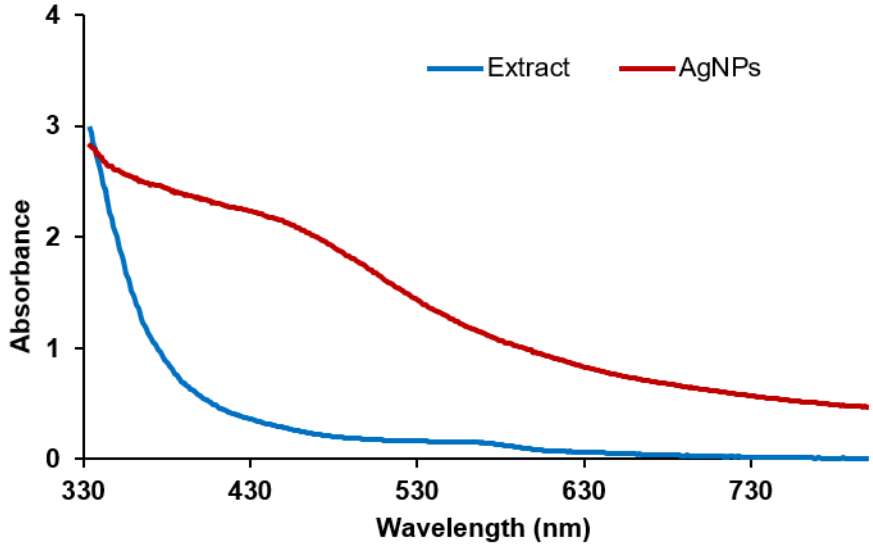

Fig. 1. UV–vis spectra of *Mercurialis annua* plant extract and AgNPs synthesized from the extract

The spectrum recorded by FTIR for the plant extract (Fig. 2) exhibited a broad and intense peak in the 3300 to 3500 cm^{-1} range, which typically refers to –OH (hydroxyl) groups. The band is related to antioxidant structures, such as phenolic compounds or flavonoids. In the silver nanoparticles, a reduction or shift of peaks within this absorption band was observed. This finding suggests that hydroxyl groups are involved in the reduction of silver ions or their binding to the nanoparticle surface. Weak bands appearing near 2900 cm^{-1} suggest C–H (alkyl) stretching vibrations, while peaks corresponding to carbonyl (C=O) and aromatic C=C bonds were detected in the 1600 to 1700 cm^{-1} range. A slight shift in this region of the nanoparticle is indicative of the involvement of carbonyl or

aromatic groups in binding to the AgNP surface. Peaks that have been observed at frequencies ranging between 1000 and 1300 cm^{-1} are commonly held to be indicative of C–O, C–N, or C–H vibrations. The weakening or shifting of bands observed in this region in the nanoparticle spectrum points to the involvement of C–O or C–N groups in surface coating or reduction reactions. In addition, the presence of weak and indistinct peaks in the 500 to 600 cm^{-1} range is indicative of metal–ligand bonds, such as Ag–O and Ag–N, supporting the generation of AgNPs (He *et al*. 2013; Azwatul *et al*. 2023).

In the FTIR profile of the AgNPs, several peaks exhibited reduced intensity or noticeable shifts, indicating interactions between the functional groups and silver ions. These results indicate that phenolic and flavonoid species within the extract may participate in Ag^{+} ion reduction and nanoparticle stabilization. As reported in a comparable study, the FTIR spectrum of *Spirogyra* sp. extract contained a broad absorption region between 3500 and 3200 cm^{-1} and a peak at 3264 cm^{-1} associated with –OH groups (Başoğlu and Akar 2023). This observation may be indicative of the occurrence of functional moieties, including –OH groups, which are commonly associated with phenolic compounds.

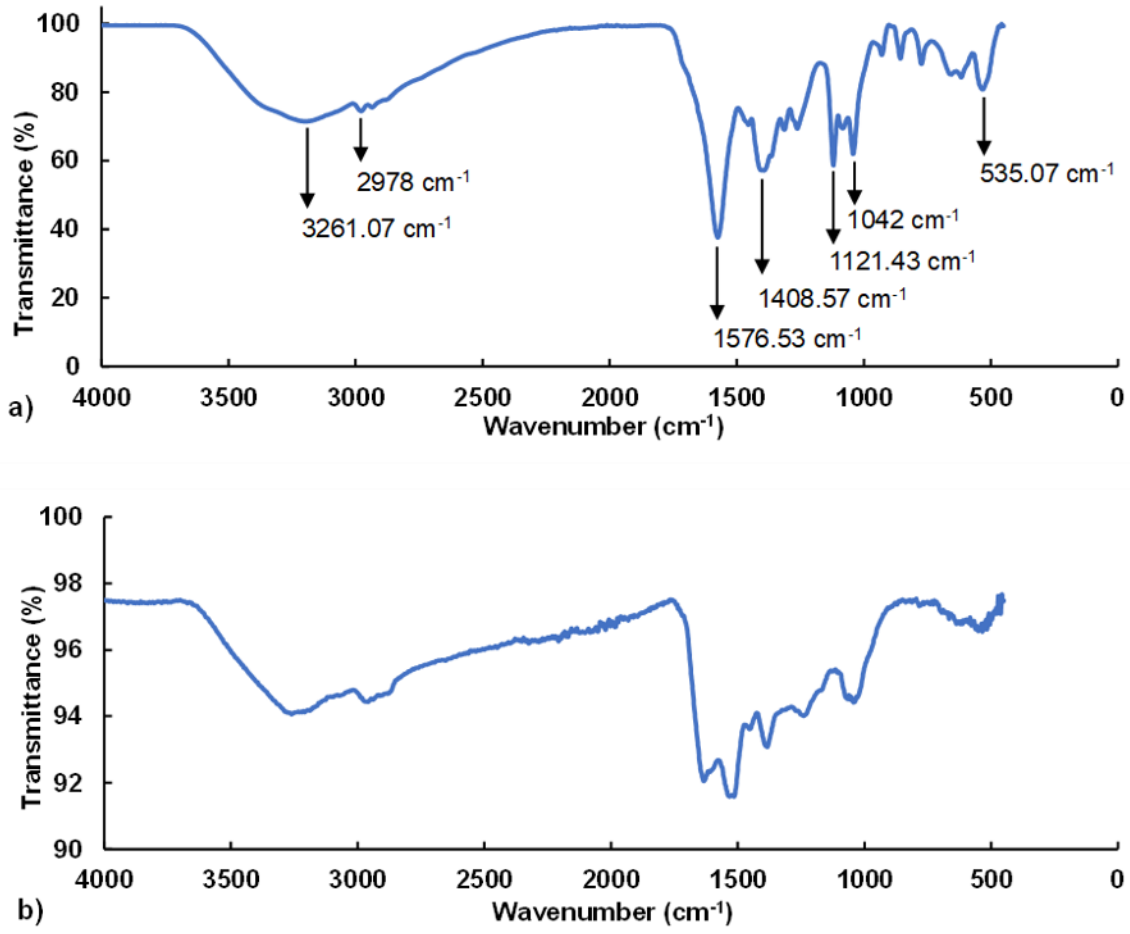

Fig. 2. FTIR profiles of the *Mercurialis annua* extract (a) and the synthesized AgNPs (b)

X-ray diffraction is a commonly applied instrumental method for examining molecular arrangements as well as crystalline structures (Bunaciu *et al*. 2015). The XRD analysis of the synthesized AgNPs characterized their crystal structure. As illustrated in

Fig. 3, the XRD pattern revealed peaks at 2θ = 38.2°, 44.5°, 64.6°, and 77.4°, which correspond to crystal planes (111), (200), (220), and (311), respectively. The results obtained from the present study indicate that the AgNPs possess a face-centered cubic (FCC) crystal structure. Furthermore, the material under discussion has been shown to demonstrate compatibility with JCPDS card no. 04-0783, as evidenced by the extant literature (Doddamani *et al.* 2023). Additional reflections were observed in the XRD pattern at 2θ = 27.3°, 29.8°, 33.0°, 43.2°, and 54.5°. Similar extra peaks have also been reported for green-synthesized AgNPs; for instance, Dangi *et al*. (2020) observed additional reflections at approximately 27.27°, 31.66°, and 45.74° for AgNPs synthesized using *Berberis asiatica* Roxb. ex DC. Although the exact peak positions may differ between studies, such minor reflections are commonly attributed to contributions from the bio-organic capping layer and/or the presence of silver oxide phases formed by partial oxidation of silver. Similarly, a green synthesis approach using *Limonia acidissima* L. reported additional XRD peaks for Ag and Ag_2O nanoparticles at 2θ values of 31.93° and 54.70°, attributed to silver oxide nanoparticles, together with further reflections around 27.65° and 45.95° (Pawar *et al*. 2016). The results of this study align with earlier literature reports that have also detected similar diffraction peaks (Vanaja and Annadurai 2013; Shruthi *et al*. 2017; Garibo *et al*. 2020).

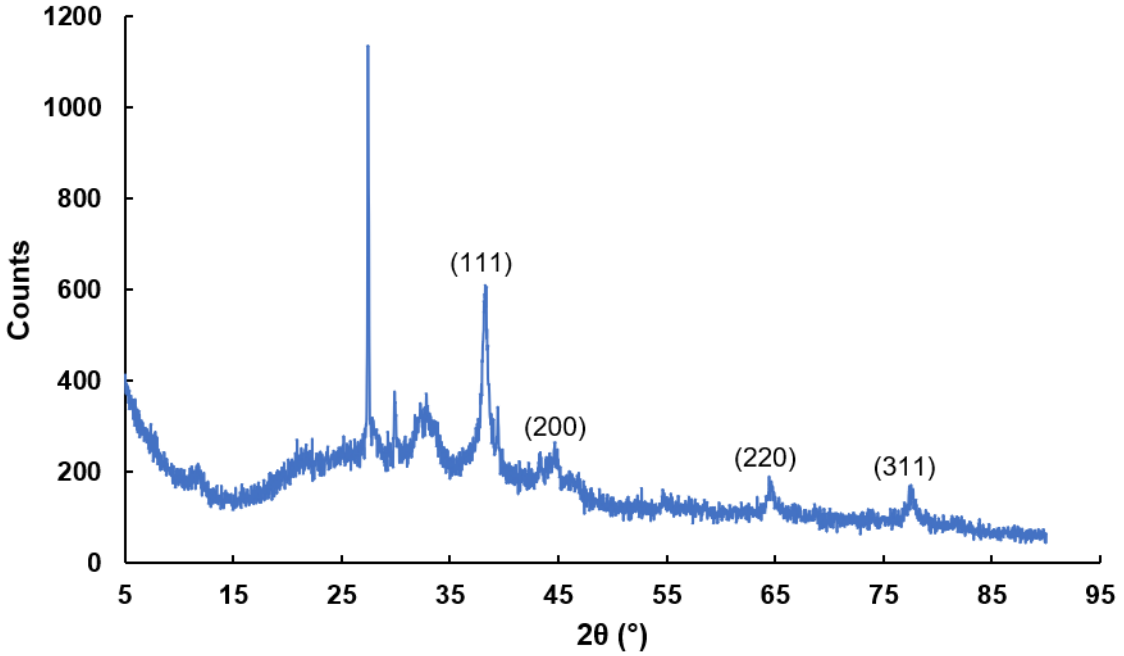

Fig. 3. XRD analysis of silver nanoparticle of *Mercurialis annua*

The TEM images indicated that the AgNPs were predominantly spherical, with most particles falling within the 10 to 30 nm size range, although occasional larger aggregates were also present. These morphological features indicate that biological synthesis occurred through a controlled process and that the particles exhibit a homogeneous distribution. These morphological characteristics are consistent with those of nanoparticles produced *via* biological (green) synthesis. In comparison, AgNPs synthesized using *Cassi occidentalis* L. were reported to range from 6.44 to 28.50 nm, exhibiting a broader size distribution (Arya *et al*. 2024).

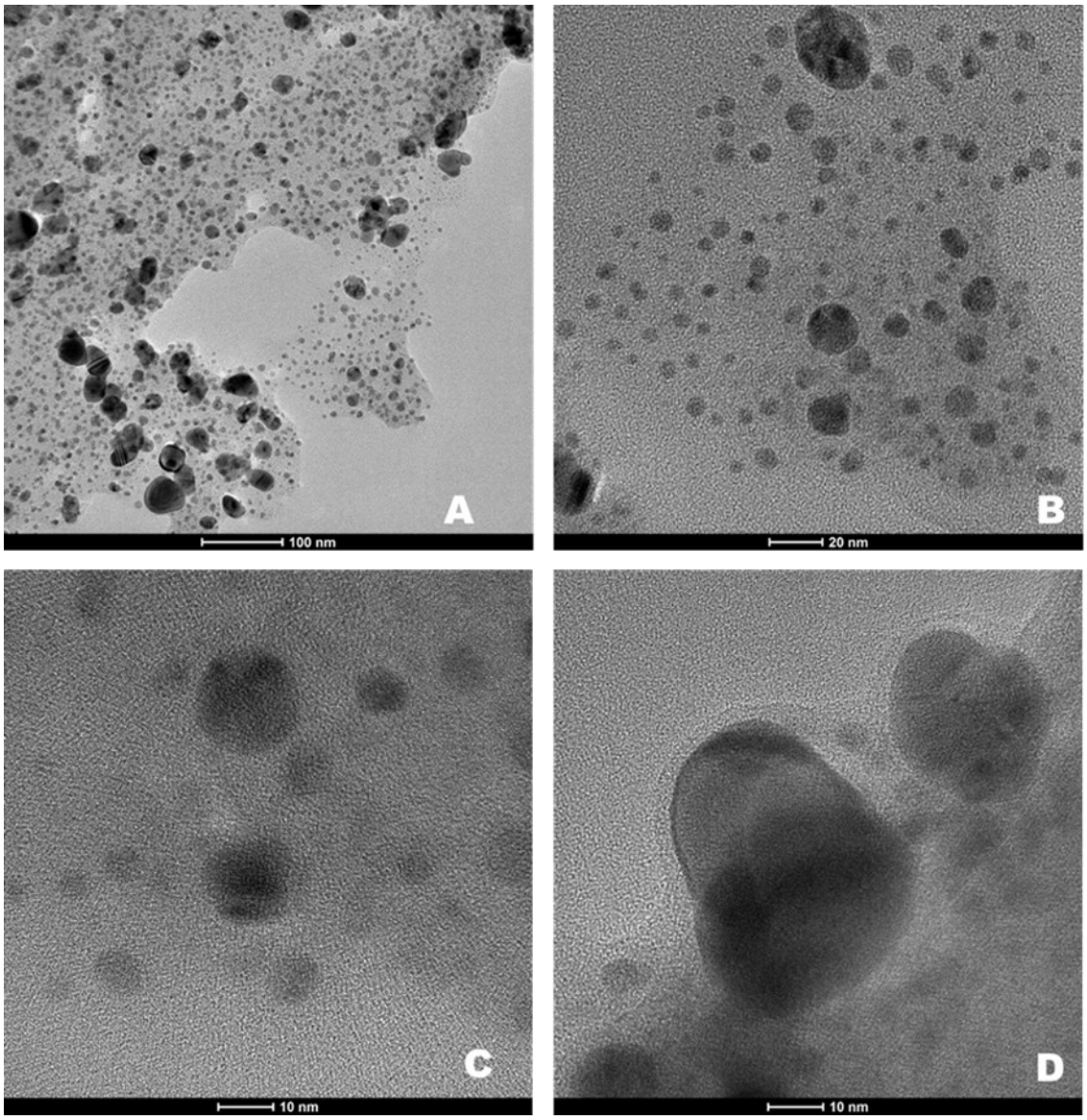

Fig. 4. TEM micrographs of AgNPs produced with *Mercurialis annua* extract, shown at various magnifications (A – D)

The EDX analysis provided information on the elemental profile of the synthesized nanoparticles. According to the quantitative EDX results, the element silver (Ag) was detected in the sample at atomic and weight percentages of 0.82%, and 6.72%, in that order. A distinct Ag–Lα signal appearing near 3 keV in the EDX profile provided evidence that metallic silver was incorporated into the nanoparticles, *i.e.*, their successful production (Dangi *et al*. 2020; Gwada *et al*. 2025). The presence of the C (86.04%), O (5.10%), and Cl (2.14%) elements were determined. The presence of these elements suggests that organic components originating from the plant extract may have been present as surface-associated phases on the nanoparticles. AgNPs have been reported to display varying concentrations of elements, such as C, O, and Cl, in addition to silver, in their EDX spectra. These variations are thought to be associated with differences in synthesis methods, reaction conditions, and the chemical composition of the plant extract used (Palithya *et al*. 2021).

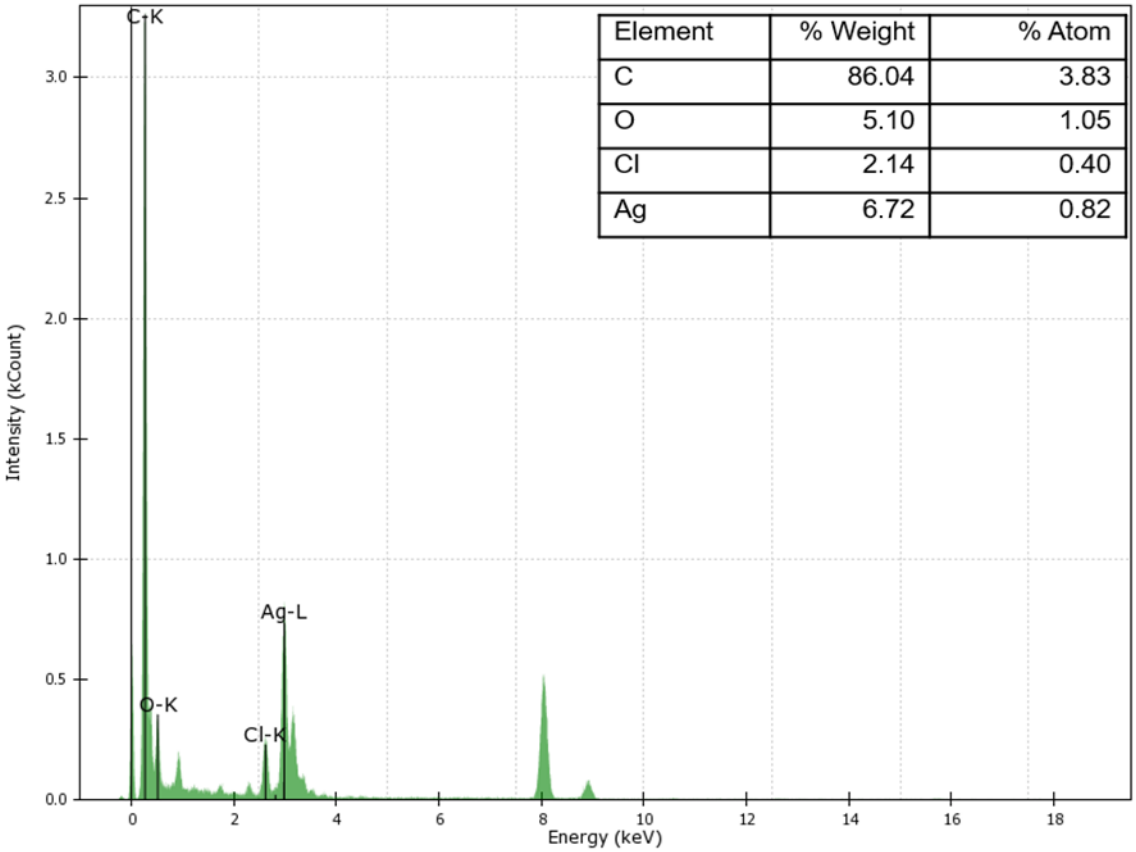

Element	% Weight	% Atom
C	86.04	3.83
O	5.10	1.05
Cl	2.14	0.40
Ag	6.72	0.82

Fig. 5. EDX spectrum and quantitative elemental composition of the biosynthesized AgNPs

Biological Activities of the Plant Extract and Nanoparticles

Antioxidant activity

The antioxidant potential of both the *M. annua* extract and its corresponding plant-derived AgNPs was assessed using the DPPH, FRAP, and CUPRAC methods. Moreover, TPC and TFC measurements were recorded to evaluate the extent to which these compounds influence antioxidant performance. Additionally, the inhibitory activities of α-glucosidase and carbonic anhydrase were examined to provide a more comprehensive assessment of the biological properties of both samples (Table 1).

In the DPPH assay, the SC_{50} value of the AgNPs was 0.059 mg/mL, compared with 0.295 mg/mL for the plant extract. These findings indicate that the nanoparticles exhibited a higher free radical scavenging activity relative to the extract. Similar observations have been reported previously. For instance, Khane *et al*. (2022) documented an IC_{50} measurement of 0.04256 mg/mL for AgNPs synthesized using *Citrus limon* (L.) Burm.f. peel extract, whereas the extract itself exhibited an IC_{50} measurement of 0.084 mg/mL. This approximate twofold difference in activity indicates that nanoparticle formation significantly enhances the antioxidant capacity in comparison with the corresponding plant extract, a trend that has been consistently observed in related studies. Supporting this pattern, Yousaf *et al*. (2020) determined that nanoparticles derived from the methanolic extract of *Achillea millefolium* L. exhibited an IC_{50} of 7.03 ± 0.31 µg/mL (0.00703 mg/mL) against the DPPH radical. For comparison, the reference antioxidant ascorbic acid (vitamin C) exhibited an IC_{50} of 4.29 ± 1.74 µg/mL (0.00429 mg/mL). These findings further substantiate the high antioxidant capacity of biosynthesized AgNPs. The findings obtained

in this study show that, regardless of the plant source used, the nanoparticle configuration consistently enhances the antioxidant effect.

Table 1. Antioxidant Potential and Enzyme Inhibition of the Extract and AgNPs

Activity Tests	Standard	Extract	AgNP
DPPH [SC_{50} (mg/mL)]	Trolox (0.0003)	0.295 ± 0.09	0.059 ± 0.03*
FRAP [TEAC (µM)]	-	228 ± 0.12	473 ± 0.18*
CUPRAC [TEAC (µM)]	-	0.023 ± 0.01	0.081 ± 0.04*
TPC [GAE(µg/mL)]	-	21.12 ± 0.15	121.55 ± 0.19*
TFC [QAE (µg/mL)]	-	0.002 ± 0.01	0.061 ± 0.02*
α-Glucosidase [IC_{50} (mg/mL)]	Acarbose (0.007)	0.183 ± 0.05	0.082 ± 0.03*
Carbonic anhydrase [IC_{50} (mg/mL)]	Sulfanilamide (0.0006)	0.245 ± 0.08	0.1454 ± 0.06*

Values are expressed as mean ± standard deviation (n = 3). Statistical comparisons between extract and AgNP samples were performed using Student's t-test. * indicates statistically significant difference compared to extract ($p < 0.05$).

The FRAP assay is a widely used method that relies on single-electron transfer to assess antioxidant capacity. The principal reaction of the assay is the transformation of the Fe^{3+}–TPTZ complex to its Fe^{2+} form within an acidic environment. Antioxidant compounds present in the sample donate electrons to the ferric complex, resulting in the formation of an intense blue-colored ferrous–TPTZ complex, which is quantitatively measured spectrophotometrically (Antolovich *et al*. 2002). In accordance with the data presented in Table 1, silver nanoparticles showed a TEAC value of 473 µM, while the plant extract exhibited a weaker activity of 228 µM. This indicates that AgNPs had approximately twice the ferric ion–reducing power of the extract. These results support the view that plant-derived compounds interacting at the nanoparticle interface help improve the overall antioxidant response. In a similar investigation, Erenler *et al*. (2021) reported FRAP values of 2.8 µmol TE/mg extract for AgNPs and 0.8 µmol TE/mg for the *Tagetes erecta* L. extract. Additionally, Alsareii *et al*. (2022) determined that AgNPs derived from *Rhizophora apiculata* Blume exhibited significantly elevated antioxidant activity, with an observed value of 1.81 ± 0.02 compared to the plant extract (0.86 ± 0.02) and the reference antioxidant ascorbic acid (1.46 ± 0.03). A comparable increase was also observed in the present study for *M. annua*, where AgNPs displayed higher ferric-reducing capacity than the plant extract.

Using the CUPRAC assay, the TEAC associated with the silver nanoparticles was determined as 0.081 µM (Table 1). The corresponding value obtained from the plant extract was 0.023 µM. The difference between the TEAC values indicates a higher cupric-reducing response for the nanoparticles under the assay conditions. The strong correlation between CUPRAC and silver nanoparticle antioxidant capacity (SNPAC) reported by Flieger *et al*. (2021) underscores the central influence of phenolic constituents on both the reducing capacity of plant extracts and the redox behavior of the resulting silver nanoparticles. The elevated TEAC value obtained for the nanoparticles produced in this work provides quantitative evidence to support this phenolic-driven relationship. This finding indicates that the phenolic constituents of the extract supported the conversion of Ag^{+} ions during nanoparticle formation and also contributed to the stronger antioxidant performance observed in the final AgNPs. This improvement has also been highlighted in studies comparing the antioxidant strength of AgNPs with other standard antioxidants. For instance, Chatterjee *et al*. (2024) assessed the antioxidant capacity of AgNPs against commonly used synthetic antioxidants, including BHA and BHT. They reported that 1 µg

of BHT and BHA corresponded to 0.63 and 1.35 µg of Trolox equivalent, respectively, whereas AgNPs reached 23.0 µg at the same concentration, indicating substantially higher antioxidant capacity.

The TPC was found to be 121.6 µg/mL GAE for the AgNP synthesized from the plant, compared to 21.1 µg/mL GAE for the plant extract (Table 1) indicating that the nanoparticles contain approximately 5.7-fold higher phenolic content of the extract. As reported by Kiani *et al*. (2023), AgNPs produced from various plant materials, such as potato peel and coriander stem likewise exhibited markedly higher phenolic content than their corresponding extracts. AgNPs derived from potato peel showed 59 ± 0.10 mg GAE/g TPC compared to 24.41 ± 0.18 mg GAE/g in the crude extract, while coriander stem-based AgNPs reached 54.65 ± 0.21 mg GAE/g, exceeding the control extract value of 21.93 ± 0.37 mg GAE/g. These findings demonstrate a consistent trend across different plant sources, indicating that nanoparticle synthesis promotes the accumulation and surface adsorption of phenolic compounds. This high rate of increase indicates that the synthesis process selectively concentrates phenolic compounds in the nanoparticle structure and enhances their potential antioxidant properties. In contrast, Sharifi-Rad *et al*. (2020) reported that at the maximum concentration tested (500 µg/mL), the extract obtained from the root of *Astragalus tribuloides* Delile contained a higher phenolic level (163.2 ± 2 µg GAE) than the AgNPs synthesized under identical conditions (106.4 ± 1 µg GAE). Makarov *et al*. (2014) highlighted the selective involvement of plant-derived metabolites in the bio reductive and stabilizing steps involved in nanoparticle generation. Consequently, it can be inferred that only a fraction of the phenolic constituents participates in nanoparticle formation, whereas a substantial portion remains in the extract, which is consistent with cases where the extract exhibits higher phenolic levels than the resulting AgNPs.

The total flavonoid concentration (TFC) in the nanoparticles was 0.061 µg/mL QAE, while in the extract this value was measured as 0.002 µg/mL QAE (Table 1). The results of the study show that the majority of flavonoid compounds bind to the surface of nanoparticle and play an active role in the synthesis process. The ability of flavonoids to reduce metal ions facilitates nanoparticle formation, while their surface binding tendencies ensure colloidal stability (Afonso *et al*. 2024). Similar results have been recorded in the literature. For example, in *Cassia auriculata* L., the flavonoid content of nanoparticles reached 891 µg QAE/mg, exceeding the values observed in the aqueous (808), ethanol (726), ethyl acetate (569), and hexane (390) extracts. However, Tyagi *et al.* (2021) found that in *Tagetes erecta* L., the flavonoid content of the extract (15.43 ± 0.34 mg QE/mL) was higher than that of the AgNP solution (8.05 ± 2.42 mg QE/mL), indicating that not all flavonoids participate in nanoparticle formation and that a portion may remain in the reaction medium or bind insufficiently to the nanoparticle surface.

Enzyme inhibition activities

The alpha-glucosidase enzyme plays a critical role in non-insulin-based diabetes therapeutic approaches, as it catalyzes the final step in carbohydrate digestion. Inhibiting this enzyme slows glucose absorption and helps lower blood sugar levels (Kardil *et al*. 2024). In inhibitor analysis performed on this enzyme, the value of IC50 in silver nanoparticles was measured as 0.082 mg/mL, while that of the plant extract was 0.183 mg/mL. The value of the standard inhibitor acarbose, used as a positive control, was 0.007 mg/mL (Table 1). Başoğlu and Akar (2023) reported that the inhibition of α-glucosidase increased from a measured level of 44.7% for the algal species *Spirogyra* sp. extract to a

higher inhibition rate of 63.5% when silver nanoparticles were used. This enhanced inhibitory effect is likely due to the expanded reactive surface provided by the nanoparticles, enabling more effective interaction with the enzyme. Sher *et al*. (2025) also provided supporting evidence, demonstrating that both *Asparagus officinalis* L. extract and its corresponding silver nanoparticles (AO-AgNPs) inhibited α-glucosidase activity. The highest inhibition was observed at 35 µg/mL: 78.7 ± 1.05% for the extract, 85.3 ± 0.65% for AO-AgNPs, and 89.6 ± 0.88% for metformin. These results suggest that AO-AgNPs have a stronger inhibitory effect than the plant extract and are comparable to the standard drug. Das *et al*. (2020) reported similar results, finding that AgNPs synthesized from various plant sources exhibited significant antidiabetic potential along with their antioxidant and cytotoxic properties.

Carbonic anhydrase (CA) is a critical enzyme that plays a key role in a multitude of physiological processes. Carbonic anhydrase inhibitors (CAIs) are widely used as therapeutic agents in various clinical conditions, particularly obesity and glaucoma (Supuran 2012). Therefore, the identification of new natural sources of CA inhibitors is of significant scientific value. A direct comparison of the extract and the produced silver nanoparticles was made to assess their carbonic anhydrase inhibitory activity. The IC_{50} measured for the nanoparticles was 0.1454 mg/mL, whereas that of the extract was 0.2451 mg/mL. The sulfanilamide standard showed an IC_{50} of 0.0006 mg/mL (Table 1), indicating the expected high potency of the positive control. Taken together, these values indicate that silver nanoparticles inhibited the enzyme more effectively than the extract. In agreement with the stronger inhibitory activity observed for silver nanoparticles, Bawazeer (2025) reported that while the methanolic extract of *Operculina turpethum* (Linn.) Silva Manso inhibited the enzyme 45.1%, the green-synthesized silver nanoparticles achieved 85.09% inhibition. The nanoparticles exhibited a low IC_{50} of 0.66 ± 0.80 µg/mL. This reflects their high potency, as lower concentrations were sufficient to suppress enzyme activity.

LC-MS/MS Analysis

The phenolic profile of the *M. annua* extract was analyzed by LC-MS/MS. In this assessment, 31 standard phenolic compounds were quantified, including prothecatechuic aldehyde, sesamol, ellagic acid, 4-hydroxybenzoic acid, prothecatechuic acid, taxifolin, gallic acid, ferulic acid, caffeic acid, resveratrol, p-coumaric acid, flavone, luteolin, chrysin, galangin, hesperidin, vanillin, luteolin-7-glucoside, catechin, gentisic acid, epicatechin, quercetin, syringic acid, rosmarinic acid, salicylic acid, oleuropein, pinocambrin, rutin, apigenin, naringenin, and chlorogenic acid. The concentrations of individual phenolic compounds, expressed in parts per million (µg/mL), are presented in Table 2. The extract contained the following phenolic acids: caffeic acid (2.24 µg/mL), ferulic acid (510 µg/mL), salicylic acid (3.14 µg/mL), and 4-hydroxybenzoic acid (3.56 µg/mL). In total, the extract's phenolic content was determined as 519 µg/mL.

Table 2. Phenolic Content of *Mercurialis annua* Plant Extract by LC–MS/MS

Phenolic Compound	Extract (µg/mL)
Caffeic acid	2,243
Ferulic acid	509,931
Salicylic acid	3,137
4-hydroxybenzoic acid	3,565
TOTAL	**518,876**

A review of the relevant literature indicates that plants contain diverse phenolic constituents, and the qualitative and quantitative characteristics of these compounds play a critical role in determining biological activity. For instance, Gecer (2025) recorded high levels of chlorogenic acid (0.55 mg/g extract), shikimic acid (3.97 mg/g extract), chrysin (2.67 mg/g extract), and scutellarin (8.67 mg/g extract) in the aqueous extract of *Centaurea saligna* (K.Koch) Wagenitz. Similarly, analysis of the ethanolic extract of *Astragalus armatus* Willd. identified 16 phenolic metabolites, with hesperidin, hyperoside, protocatechuic acid, 4-hydroxybenzoic acid, rosmarinic acid, and chlorogenic acid occurring at comparatively higher levels (Lekmine *et al.* 2022). These variations in phenolic composition can be attributed to species-specific secondary metabolite profiles. Overall, the chemical composition of plant extracts differs substantially among species, contributing to their distinct biological potentials. In the present study, ferulic acid was identified as the predominant phenolic compound in the *M. annua* extract, which is of particular significance. It has been reported that ferulic acid functions as a reducing agent during the synthesis of AgNPs, contributing to nanoparticle stabilization and enhancing their biological activity (Li *et al*. 2024). In addition to its role in nanoparticle synthesis, ferulic acid also exhibits biological activity through the inhibition of α-glucosidase *via* non-covalent interactions (Zheng *et al*. 2020). Caffeic, salicylic, and 4-hydroxybenzoic acids were detected at lower concentrations in the present study; these compounds have been shown to exhibit biological activity. For example, caffeic acid has been shown to exhibit biological activity in a nanoparticle system (Choi *et al*. 2017), while salicylic (Wang *et al*. 2015) and 4-hydroxybenzoic acid (López-Herrador *et al*. 2025) contribute to antioxidant-related biological activity.

The biological activity of nanoparticle systems may be attributed to the synergistic interactions of their constituents as well as their enhanced bioavailability (Flieger *et al*. 2021). Accordingly, biosynthesized nanoparticles derived from plant extracts offer significant potential for further biomedical exploration.

CONCLUSIONS

1. The formation and structural properties of the silver nanoparticles were verified through Fourier transform infrared (FTIR), X-ray diffraction (XRD), UV–Vis, transmission electron microscopy (TEM), and energy-dispersive X-ray (EDX) analyses after they were successfully synthesized from the aerial parts of *M. annua* in this study.
2. The characterization results showed that the nanoparticles displayed mainly spherical morphology, a nanometre-scale crystalline silver structure, and surface stabilization mediated by extract-derived functional groups.
3. In the biological activity assessments, the nanoparticles showed higher antioxidant activity than the extract in all parameters.
4. The enzyme inhibition results were consistent with this pattern, revealing that the nanoparticles exerted stronger inhibitory effects on both α-glucosidase and carbonic anhydrase.
5. The liquid chromatography/mass spectrometry (LC-MS/MS) analysis identified 31 phenolic compounds in the extract, with ferulic acid, caffeic acid, salicylic acid, and 4-

hydroxybenzoic acid present in comparatively high amounts, and the total phenolic concentration was determined as 518.876 µg/mL.

6. The biosynthesized silver nanoparticles from the aerial parts of the *Mercurialis annua* plant using the green synthesis method may be a potentially valuable material for biomedical and pharmaceutical applications, particularly as antioxidant and enzyme inhibitor agents. However, further studies are required to assess the safety and practical applicability of these nanoparticles, including evaluations of cellular toxicity, biocompatibility, and *in vivo* performance.

ACKNOWLEDGMENTS

The authors would like to thank Dr. Bülent Akar for his assistance in the collection and identification of plant materials, and Dr. Uğur Kardil for his support in the laboratory studies on carbonic anhydrase enzyme activity.

Conflict of Interest

The authors of this work declare that they have no conflicts of interest.

Use of Generative AI

Generative AI tools (ChatGPT, OpenAI, GPT-5.2 model) were used only for language editing and improving textual clarity. No generative AI tools were used for data analysis, interpretation of results, preparation of visuals (figures, graphics, diagrams), scientific content creation, or reference compilation. All scientific content, findings, and conclusions were produced entirely by the authors.

REFERENCES CITED

Afonso, I. S., Cardoso, B., Nobrega, G., Minas, G., Ribeiro, J. E., and Lima, R. A. (2024). "Green synthesis of nanoparticles from olive oil waste for environmental and health applications: A review," *Journal of Environmental Chemical Engineering* 12(5), article 114022. https://doi.org/10.1016/j.jece.2024.114022

Ahmed, S., Ahmad, M., Swami, B. L., and Ikram, S. (2016). "A review on plants extracts mediated synthesis of silver nanoparticles for antimicrobial applications: A green expertise," *Journal of Advanced Research* 7(1), 17-28. https://doi.org/10.1016/j.jare.2015.02.007

Akar, Z., Karakurt, A., Okumus, F., Cinemre, S., Duzgun, A. O., Akar, B., and Can, Z. (2020). "RP-HPLC-UV analysis of the phenolic compounds, antimicrobial activity against multi-drug resistant bacteria and antioxidant activity of fruit and seed of *Diospyros lotus* L." *International Journal of Secondary Metabolites* 7(4), 237-246. https://doi.org/10.21448/ijsm.714108

Akar, Z., Akay, S., Ejder, N., and Özad Düzgün, A. (2024). "Determination of the cytotoxicity and antibiofilm potential effect of *Equisetum arvense* silver nanoparticles," *Applied Biochemistry and Biotechnology* 196(2), 909-922. https://doi.org/10.1007/s12010-023-04587-7

Akar, Z., Demir, Ç., Alkan, O., Can, Z., and Akar, B. (2021). "LC–MS/MS and RP–HPLC–UV analysis and antioxidant activities of *Arum italicum* Miller edible and nonedible tuber parts," *Journal of Anatolian Environmental and Animal Sciences* 6(3), 294-301. https://doi.org/10.35229/jaes.864484

Aktepe, N., Baran, A., and Keskin, C. (2025a). "Cytotoxic and antimicrobial analysis of biosynthesized selenium nanoparticles from *Solanum tuberosum* peels," *International Journal of Agriculture Environment and Food Sciences* 9(2), 559-569. https://doi.org/10.31015/2025.2.29

Aktepe, N., Baran, A., Baran, M. F., Öziç, C., Karadağ, M., and Atalar, M. N. (2025b). "Phenolic analysis and antimicrobial potential of *Glycyrrhiza glabra* L. plant root extract," *MAS Journal of Applied Sciences* 10(4), 717-727. https://doi.org/10.5281/zenodo.17797771

Alan, F., and Çolak, A. M. (2025). "Phytochemical and antioxidant characterization of myrtle (*Myrtus communis* L.) fruit," *ISPEC Journal of Agricultural Sciences* 9(4), 1182-1193. https://doi.org/10.5281/zenodo.17928995

Alsareii, S. A., Alamri, A. M., AlAsmari, M. Y., Bawahab, M. A., Mahnashi, M. H., Shaikh, I. A., Shettar, A. K., Hoskeri, J. H., and Kumbar, V. (2022). "Synthesis and characterization of silver nanoparticles from *Rhizophora apiculata* and studies on their wound healing, antioxidant, anti-inflammatory, and cytotoxic activity," *Molecules* 27(19), article 6306. https://doi.org/10.3390/molecules27196306

Antolovich, M., Prenzler, P. D., Patsalides, E., McDonald, S., and Robards, K. (2002). "Methods for testing antioxidant activity," *The Analyst* 127, 183–198. https://doi.org/10.1039/B009171P

Apak, R., Güçlü, K., Özyürek, M., and Karademir, S. E. (2004). "Novel total antioxidant capacity index for dietary polyphenols and vitamins C and E, using their cupric ion reducing capability in the presence of neocuproine: CUPRAC method," *Journal of Agricultural and Food Chemistry* 52(24), 7970-7981. https://doi.org/10.1021/jf048741x

Armstrong, P. J., and Frederick, C. O. (1966). *A Mathematical Representation of the Multiaxial Bauschinger Effect* (Vol. 731), Berkeley Nuclear Laboratories, Berkeley, CA, USA.

Arya, A., Tyagi, P. K., Bhatnagar, S., Bachheti, R. K., Bachheti, A., and Ghorbanpour, M. (2024). "Biosynthesis and assessment of antibacterial and antioxidant activities of silver nanoparticles utilizing *Cassia occidentalis* L. seed," *Scientific Reports* 14, article 7243. https://doi.org/10.1038/s41598-024-57823-3

Azwatul, H. M., Uda, M. N. A., Gopinath, S. C. B., Arsat, Z. A., Abdullah, F., Muttalib, M. F. A., Hashim, M. K. R., Hashim, U., Isa, M., Uda, M. N. A., *et al.* (2023). "Plant-based green synthesis of silver nanoparticle via chemical bonding analysis," *Materials Today: Proceedings*, in press. https://doi.org/10.1016/j.matpr.2023.01.005

Başoğlu, A., and Akar, Z. (2023). "Green biosynthesis, characterization of silver nanoparticles using a green alga *Spirogyra* sp., and their antioxidant and enzyme activities," *International Advanced Research and Engineering Journal* 7(1), 41-45. https://doi.org/10.35860/iarej.1180456

Bawazeer, S. (2025). "Green synthesis: An eco-friendly approach for the synthesis of silver nanoparticles functionalized with *Operculina turpethum* and its *in vitro* and *in vivo* biological activities," *International Journal of Nanomedicine* 20, 2991-3005. https://doi.org/10.2147/IJN.S507134

Benzie, I. F. F., and Strain, J. J. (1996). "The ferric reducing ability of plasma (FRAP) as a measure of 'antioxidant power': The FRAP assay," *Analytical Biochemistry* 239, 70-76. https://doi.org/10.1006/abio.1996.0292

Brand-Williams, W., Cuvelier, M. E., and Berset, C. L. W. T. (1995). "Use of a free radical method to evaluate antioxidant activity," *LWT – Food Science and Technology* 28(1), 25-30. https://doi.org/10.1016/S0023-6438(95)80008-5

Bunaciu, A. A., Udriștioiu, E. G., and Aboul-Enein, H. Y. (2015). "X-ray diffraction: Instrumentation and applications," *Critical Reviews in Analytical Chemistry* 45(4), 289-299. https://doi.org/10.1080/10408347.2014.949616

Cardoso, B., Nobrega, G., Afonso, I. S., Ribeiro, J. E., and Lima, R. A. (2025). "Sustainable green synthesis of metallic nanoparticle using plants and microorganisms: A review of biosynthesis methods, mechanisms, toxicity, and applications," *Journal of Environmental Chemical Engineering* 13(3), article 116921. https://doi.org/10.1016/j.jece.2025.116921

Chatterjee, N., Pal, S., and Dhar, P. (2024). "Green silver nanoparticles from bacteria—Antioxidant, cytotoxic and antifungal activities," *Next Nanotechnology* 6, article 100089. https://doi.org/10.1016/j.nxnano.2024.100089

Choi, K. H., Nam, K. C., Lee, S. Y., Cho, G., Jung, J. S., Kim, H. J., and Park, B. J. (2017). "Antioxidant potential and antibacterial efficiency of caffeic acid-functionalized ZnO nanoparticles," *Nanomaterials* 7(6), article 148. https://doi.org/10.3390/nano7060148

Dangi, S., Gupta, A., Gupta, D. K., Singh, S., and Parajuli, N. (2020). "Green synthesis of silver nanoparticles using aqueous root extract of *Berberis asiatica* and evaluation of their antibacterial activity," *Chemical Data Collections* 28, article 100411. https://doi.org/10.1016/j.cdc.2020.100411

Das, G., Shin, H.-S., and Patra, J. K. (2020). "Comparative assessment of antioxidant, anti-diabetic and cytotoxic effects of three peel/shell food waste extract-mediated silver nanoparticles," *International Journal of Nanomedicine* 15, 9075-9088. https://doi.org/10.2147/IJN.S277625

Doddamani, T., Balasubramanian, B., Kakkalameli, S., Kadanthottu Sebastian, J., Pappuswamy, M., Almutairi, B. O., Almutairi, M. H., and Daphedar, A. (2025). "Phytofabricated silver nanoparticles derived from *Leea crispa* leaf extract: Antituberculosis and anticancer activities," *BioResources* 20(1), 452-464. https://doi.org/10.15376/biores.20.1.452-464

Erenler, R., Geçer, E. N., Genç, N., and Yanar, D. (2021). "Antioxidant activity of silver nanoparticles synthesized from *Tagetes erecta* L. leaves," *International Journal of Chemistry and Technology* 5(2), 141-146. https://doi.org/10.32571/ijct.1005275

Flieger, J., Franus, W., Panek, R., Szymańska-Chargot, M., Flieger, W., Flieger, M., and Kołodziej, P. (2021). "Green synthesis of silver nanoparticles using natural extracts with proven antioxidant activity," *Molecules* 26(16), article 4986. https://doi.org/10.3390/molecules26164986

Fukumoto, L. R., and Mazza, G. (2000). "Assessing antioxidant and prooxidant activities of phenolic compounds," *Journal of Agricultural and Food Chemistry* 48(8), 3597-3604. https://doi.org/10.1021/jf000220w

Garibo, D., Borbón-Nuñez, H. A., Díaz de León, J. N., García Mendoza, E., Estrada, I., Toledano-Magaña, Y., Tiznado, H., Ovalle-Marroquin, M., Soto-Ramos, A. G., Blanco, A., *et al.* (2020). "Green synthesis of silver nanoparticles using *Lysiloma*

acapulcensis exhibit high-antimicrobial activity," *Scientific Reports* 10, article 12805. https://doi.org/10.1038/s41598-020-69606-7

Gecer, E. N. (2025). "Phytochemistry of *Centaurea saligna*: Silver nanoparticle synthesis, quantification of natural compounds, antioxidant and antibacterial activity," *Scientific Reports* 15, article 26307. https://doi.org/10.1038/s41598-025-11970-3

Gwada, C. A., Ndivhuwo, P. S., Matshetshe, K., Aradi, E., Mdluli, P., Moloto, N., Otieno, F., and Airo, M. (2025). "Phytochemical-assisted synthesis, optimization, and characterization of silver nanoparticles for antimicrobial activity," *RSC Advances* 15(18), 14170-14181. https://doi.org/10.1039/d4ra08900f

Hanna, D. H., Nady, D. S., Wasef, M. W., Fakhry, M. H., Mohamed, F. S., Isaac, D. M., Kirolos, M. M., Azmy, M. S., Hakeem, G. E., and Fathy, C. A. (2025). "Plant-derived nanoparticles: Green synthesis, factors, and bioactivities," *Next Materials* 9, article 101275. https://doi.org/10.1016/j.nxmate.2025.101275

He, Y., Du, Z., Lv, H., Jia, Q., Tang, Z., Zheng, X., Zhang, K., and Zhao, F. (2013). "Green synthesis of silver nanoparticles by *Chrysanthemum morifolium* Ramat. extract and their application in clinical ultrasound gel," *International Journal of Nanomedicine* 8, 1809-1815. https://doi.org/10.2147/IJN.S43289

Henglein, A. (1993). "Physicochemical properties of small metal particles in solution: Microelectrode reactions, chemisorption, composite metal particles, and the atom-to-metal transition," *Journal of Physical Chemistry* 97(21), 5457-5471. https://doi.org/10.1021/j100123a004

Iravani, S., Korbekandi, H., Mirmohammadi, S. V., and Zolfaghari, B. (2014). "Synthesis of silver nanoparticles: Chemical, physical and biological methods," *Research in Pharmaceutical Sciences* 9(6), 385-406.

Jiang, X., Khan, S., Dykes, A., Stulz, E., and Zhang, X. (2025). "Biogenic synthesis of silver nanoparticles and their diverse biomedical applications," *Molecules* 30(15), article 3104. https://doi.org/10.3390/molecules30153104

Karakullukçu, V., Akar, B., Baltacı, C., Özad Düzgün, A., and Karpuz, Ö. (2023). "Characterization, antioxidant and antimicrobial activities of iron nanoparticles synthesized using *Firethorn* fruit (*Pyracantha coccinea* Roemer) extracts," *Karaelmas Science and Engineering Journal* 13(2), 255-265. https://doi.org/10.7212/karaelmasfen.1297963

Kardil, U., Akar, Z., and Düzgün, A. Ö. (2024). "Investigation of antibiofilm and biological activities of *Vaccinium arctostaphylos* L.," *Turkish Journal of Analytical Chemistry* 6(1), 25-31. https://doi.org/10.51435/turkjac.1489982

Khane, Y., Benouis, K., Albukhaty, S., Sulaiman, G. M., Abomughaid, M. M., Al Ali, A., Aout, D., Fenniche, F., Khane, S., Chaibi, W., *et al.* (2022). "Green synthesis of silver nanoparticles using aqueous *Citrus limon* zest extract: Characterization and evaluation of their antioxidant and antimicrobial properties," *Nanomaterials* 12, article 2013. https://doi.org/10.3390/nano12122013

Kiani, B. H., Arshad, I., Najeeb, S., Okla, M. K., Almanaa, T. N., Al-Qahrani, W. H., and Abdel-Maksoud, M. A. (2023). "Evaluation of biogenic silver nanoparticles synthesized from vegetable waste," *International Journal of Nanomedicine* 18, 6527-6544. https://doi.org/10.2147/IJN.S432252

Lekmine, S., Bendjeldi, S., Benslama, O., Martin-Garcia, A. I., Boussekine, S., Kadi, K., Akkal, S., Nieto, G., Sami, R., Al-Mushhin, A. A. M., *et al.* (2022). "Ultrasound-assisted extraction, LC–MS/MS analysis, anticholinesterase, and antioxidant activities

of valuable natural metabolites from *Astragalus armatus* Willd.: *In silico* molecular docking and *in vitro* enzymatic studies," *Antioxidants* 11(10), article 2000. https://doi.org/10.3390/antiox11102000

Li, D., Chen, L., and Qiu, X. (2024). "Rapid synthesis of ferulic acid-derived lignin coated silver nanoparticles with low cytotoxicity and high antibacterial activity," *International Journal of Biological Macromolecules* 277, article 134471. https://doi.org/10.1016/j.ijbiomac.2024.134471

López-Herrador, S., Corral-Sarasa, J., González-García, P., Morillas-Morota, Y., Olivieri, E., Jiménez-Sánchez, L., and Díaz-Casado, M. E. (2025). "Natural hydroxybenzoic and hydroxycinnamic acids derivatives: Mechanisms of action and therapeutic applications," *Antioxidants* 14(6), article 711. https://doi.org/10.3390/antiox14060711

Lorenz, P., Duckstein, S., Conrad, J., Knödler, M., Meyer, U., and Stintzing, F. C. (2012). "An approach to the chemotaxonomic differentiation of two European dog's mercury species: *Mercurialis annua* L. and *M. perennis* L.," *Chemistry and Biodiversity* 9(2), 282-297. https://doi.org/10.1002/cbdv.201100341

Makarov, V. V., Love, A. J., Sinitsyna, O. V., Makarova, S. S., Yaminsky, I. V., Taliansky, M. E., and Kalinina, N. O. (2014). "Green nanotechnologies: Synthesis of metal nanoparticles using plants," *Acta Naturae* 6(1), 35-44. https://doi.org/10.32607/20758251-2014-6-1-35-44

Ovais, M., Khalil, A. T., Islam, N. U., Ahmad, I., Ayaz, M., Saravanan, M., Shinwari, Z. K., and Rauf, A. (2018). "Role of plant phytochemicals and microbial enzymes in biosynthesis of metallic nanoparticles," *Applied Microbiology and Biotechnology* 102, 6799-6814. https://doi.org/10.1007/s00253-018-9146-7

Özçelik, B., and Kara, A. (2023). "Evaluation of biological activities of silver nanoparticles (AgNPs) synthesized by green nanotechnology from birch (*Betula* spp.) branches extract," *Turkish Journal of Analytical Chemistry* 5(2), 151-161. https://doi.org/10.51435/turkjac.1401931

Palithya, S., Gaddam, S. A., Kotakadi, V. S., Penchalaneni, J., and Challagundla, V. N. (2021). "Biosynthesis of silver nanoparticles using leaf extract of *Decaschistia crotonifolia* and its antibacterial, antioxidant, and catalytic applications," *Green Chemistry Letters and Reviews* 14(1), 137-152. https://doi.org/10.1080/17518253.2021.1876172

Pannell, J. R., Dorken, M. E., Pujol, B., and Berjano, R. (2008). "Gender variation and transitions between sexual systems in *Mercurialis annua* (Euphorbiaceae)," *International Journal of Plant Sciences* 169(1), 129-139. https://doi.org/10.1086/523360

Pawar, O., Deshpande, N., Dagade, S., Waghmode, S., and Nigam Joshi, P. (2016). "Green synthesis of silver nanoparticles from purple acid phosphatase apoenzyme isolated from a new source *Limonia acidissima*," *Journal of Experimental Nanoscience* 11(1), 28-37. https://doi.org/10.1080/17458080.2015.1025300

Rai, M., Yadav, A., and Gade, A. (2009). "Silver nanoparticles as a new generation of antimicrobials," *Biotechnology Advances* 27(1), 76-83. https://doi.org/10.1016/j.biotechadv.2008.09.002

Sharifi-Rad, M., Pohl, P., Epifano, F., and Álvarez-Suarez, J. M. (2020). "Green synthesis of silver nanoparticles using *Astragalus tribuloides* Delile root extract: Characterization, antioxidant, antibacterial, and anti-inflammatory activities," *Nanomaterials* 10(12), article 2383. https://doi.org/10.3390/nano10122383

Sharma, V. K., Yngard, R. A., and Lin, Y. (2019). "Silver nanoparticles: Green synthesis and their antimicrobial activities," *Advances in Colloid and Interface Science* 145(1–2), 83-96. https://doi.org/10.1016/j.cis.2008.09.002

Sher, A., Tsai, T.-C., Sohail, A., Alouffi, A., Almutairi, M. M., Wadood, A., Ajmal, A., Muhammad, W., Chen, C.-C., Ali, A., *et al.* (2025). "Green synthesis of silver nanoparticles and characterization using *Asparagus officinalis*: Elucidation of anti-diabetic potentials through in silico, in vitro, and in vivo analyses," *Green Chemistry Letters and Reviews* 18(1), article 2479589. https://doi.org/10.1080/17518253.2025.2479589

Shruthi, G., Prasad, K. S., Vinod, T. P., Balamurugan, V., and Shivamallu, C. (2017). "Green synthesis of biologically active silver nanoparticles through a phyto-mediated approach using *Areca catechu* leaf extract," *ChemistrySelect* 2(32), 10612-10619. https://doi.org/10.1002/slct.201702257

Singh, H., Desimone, M. F., Pandya, S., Jasani, S., George, N., Adnan, M., Hamid, M., Alnaim, A. A., and Alderhami, S. A. (2023). "Revisiting the green synthesis of nanoparticles: Uncovering influences of plant extracts as reducing agents for enhanced synthesis efficiency and its biomedical applications," *International Journal of Nanomedicine* 18, 4727-4750. https://doi.org/10.2147/IJN.S419369

Slinkard, K., and Singleton, V. L. (1977). "Total phenol analysis: Automation and comparison with manual methods," *American Journal of Enology and Viticulture* 28, 49-55. https://doi.org/10.5344/ajev.1977.28.1.49

Smitha, P. S., Sheeja, T. T., and Manju, M. (2020). "Green nanoparticles from different plant groups," in: *Phytonanotechnology: Challenges and Prospects*, N. Thajuddin and S. Mathew (eds.), Elsevier, Oxford, UK, pp. 51-70. https://doi.org/10.1016/B978-0-12-822348-2.00004-8

Supuran, C. T. (2012). "Structure-based drug discovery of carbonic anhydrase inhibitors," *Journal of Enzyme Inhibition and Medicinal Chemistry* 27(6), 759-772. https://doi.org/10.3109/14756366.2012.672983

Tekin, S. B., Poyrazoğlu, E. S., and Güçer, Y. (2025). "Investigation of the functional properties of some *Origanum s*pecies and their bioactive components," *ISPEC Journal of Agricultural Sciences* 9(2), 630-643. https://doi.org/10.5281/zenodo.15510420

Tyagi, P. K., Tyagi, S., Gola, D., Arya, A., Ayatollahi, S. A., Alshehri, M. M., and Sharifi-Rad, J. (2021). "Ascorbic acid and polyphenols mediated green synthesis of silver nanoparticles from *Tagetes erecta* L. aqueous leaf extract and their antioxidant properties," *Journal of Nanomaterials* 2021, article 6515419. https://doi.org/10.1155/2021/6515419

Vanaja, M., and Annadurai, G. (2013). "*Coleus aromaticus* leaf extract mediated synthesis of silver nanoparticles and its bactericidal activity," *Applied Nanoscience* 3, 217-223. https://doi.org/10.1007/s13204-012-0121-9

Wang, Z., Ma, L., Zhang, X., Xu, L., Cao, J., and Jiang, W. (2015). "The effect of exogenous salicylic acid on antioxidant activity, bioactive compounds and antioxidant system in apricot fruit," *Scientia Horticulturae* 181, 113-120. https://doi.org/10.1016/j.scienta.2014.10.055

Yousaf, H., Mehmood, A., Ahmad, K. S., and Raffi, M. (2020). "Green synthesis of silver nanoparticles and their applications as an alternative antibacterial and antioxidant agent," *Materials Science and Engineering C* 112, article 110901. https://doi.org/10.1016/j.msec.2020.110901

Yu, Z., Yin, Y., Zhao, W., Liu, J., and Chen, F. (2012). "Anti-diabetic activity peptides from albumin against α-glucosidase and α-amylase," *Food Chemistry* 135(3), 2078-2085. https://doi.org/10.1016/j.foodchem.2012.06.088

Zheng, Y., Tian, J., Yang, W., Chen, S., Liu, D., Fang, H., Zhang, H., and Ye, X. (2020). "Inhibition mechanism of ferulic acid against α-amylase and α-glucosidase," *Food Chemistry* 317, article 126346. https://doi.org/10.1016/j.foodchem.2020.126346

Article submitted: January 25, 2026; Peer review completed: April 4, 2026; Revised version received: May 26, 2026; Accepted: July 21, 2026; Published: August 10, 2026.
DOI: 10.15376/biores.21.4.9492-9512